4-2007

An Extended Stem-Loop 1 is Necessary for Human Immunodeficiency Virus Type 2 Replication and Affects Genomic RNA Encapsidation

Jean-Marc Lanchy

J. Stephen Lodmell

University of Montana - Missoula, stephen.lodmell@umontana.edu

JOURNAL OF VIROLOGY, Apr. 2007, p. 3285–3292 Vol. 81, No. 7
0022-538X/07/$08.00+0 doi:10.1128/JVI.02025-06

An Extended Stem-Loop 1 Is Necessary for Human Immunodeficiency Virus Type 2 Replication and Affects Genomic RNA Encapsidation[▽]

Jean-Marc Lanchy and J. Stephen Lodmell*

Division of Biological Sciences, The University of Montana, Missoula, Montana 59812

Received 15 September 2006/Accepted 5 January 2007

Genomic RNA encapsidation in lentiviruses is a highly selective and regulated process. The unspliced RNA molecules are selected for encapsidation from a pool of many different viral and cellular RNA species. Moreover, two molecules are encapsidated per viral particle, where they are found associated as a dimer. In this study, we demonstrate that a 10-nucleotide palindromic sequence (pal) located at the 3′ end of the ψ encapsidation signal is critical for human immunodeficiency virus type 2 (HIV-2) replication and affects genomic RNA encapsidation. We used short-term and long-term culture of pal-mutated viruses in permissive C8166 cells and their phenotypic reversion to show the existence of a structurally extended SL1 during HIV-2 replication, formed by the interaction of the 3′ end of the pal within ψ with a motif located downstream of SL1. The stem extending HIV-2 SL1 is structurally similar to stem B described for HIV-1 SL1. Despite the high degree of phylogenetic conservation, these results show that mutant viruses are viable when the autocomplementary nature of the pal sequence is disrupted, but not without a stable stem B. Our observations show that formation of the extended SL1 is necessary during viral replication and positively affects HIV-2 genomic RNA encapsidation. Sequestration of part of the packaging signal into SL1 may be a means of regulating its presentation during the replication cycle.

The 5′-untranslated regions of retroviral RNAs contain several structured motifs that are involved in various steps in viral replication, including transcriptional transactivation, splicing, encapsidation, dimerization, and initiation of reverse transcription (for a review, see reference 3). Encapsidation of the genomic RNA in lentiviruses is a very specific process. Two molecules of unspliced RNA are selected for encapsidation over a vast excess of different spliced viral RNA species and cellular RNA. The historical model of retroviral RNA encapsidation has been that viral structural proteins like Gag recognize and bind specific RNA motifs located downstream of the major splice donor site, and thus only present in the unspliced viral RNA, and transfer a pair of these molecules into one newly forming viral particle (for a review, see references 11 and 20).

However, most recent studies suggest that the encapsidation signal is not limited to a single RNA element. The human immunodeficiency virus type 1 (HIV-1) encapsidation signal is multipartite, with structural elements located across the 5′-untranslated and Gag-encoding regions (4, 6, 31). Similarly, HIV-2 and simian immunodeficiency virus (SIV) RNA encapsidation motifs have been localized either downstream of the major splice donor site (38), upstream (16, 32, 39, 46), or both (1, 37).

A hallmark of retroviral RNA encapsidation is that two molecules of genomic RNA are encapsidated per viral particle (for a review, see references 14, 34, and 41). Gentle extraction and deproteinization of virions revealed that the two encapsidated RNA molecules form a dimer through noncovalent RNA-RNA interactions (28). Electron microscopy studies with increasing denaturation identified the 5′ ends of the genomic RNA molecules as the location of the strongest RNA-RNA interaction in dimers isolated from viral particles; this interaction was named the dimer linkage structure (see reference 2 for the original study and reference 19 for a study with HIV-1). In HIV-1, a strong candidate involved in the formation of the dimer linkage structure was identified in vitro upstream of the major splice donor site. This element was named the dimerization initiation site or stem-loop 1 (SL1) (18, 25, 33, 35, 45). Besides its role in genomic RNA dimerization, the SL1 sequence was shown to be involved in other stages of HIV-1 replication, notably encapsidation (see Table 1 in reference 34).

We previously presented evidence that the ψ encapsidation signal interferes with SL1-mediated HIV-2 RNA dimerization in vitro (23). The sequence responsible is a 10-nucleotide (nt) palindromic sequence (pal) located at the 3′ end of ψ. The pal motif was also shown to mediate RNA dimerization upon binding of an antisense oligonucleotide directed against SL1 (23). We and others showed that the dimerization of HIV-2 leader RNA is regulated in vitro by a long-distance intramolecular interaction between nucleotides located at the 5′ end of U5 and nucleotides encompassing the *gag* translation initiation site (10, 24). Thus, several short- and long-distance interactions influence the presentation of the ψ-SL1 region in HIV-2 leader RNA in vitro.

Since the pal motif is located within the ψ encapsidation signal, is phylogenetically conserved (see Discussion), and can influence dimerization of HIV-2 leader RNA fragments in vitro, we have analyzed in this study the function of HIV-2 pal during replication in permissive C8166 cells. We also used long-term culture of defective viruses and their phenotypic reversion to gain insight into the necessity of the palindromic sequence and functionally important secondary structure interactions. In particular, we show that the defects in viral replication for some pal-mutated viruses can be compensated for by nucleotide changes in or close to the mutated pal ele-

* Corresponding author. Mailing address: Division of Biological Sciences, The University of Montana, Missoula, MT 59812. Phone: (406) 243-6393. Fax: (406) 243-4304. E-mail: stephen.lodmell@umontana.edu.

▽ Published ahead of print on 17 January 2007.

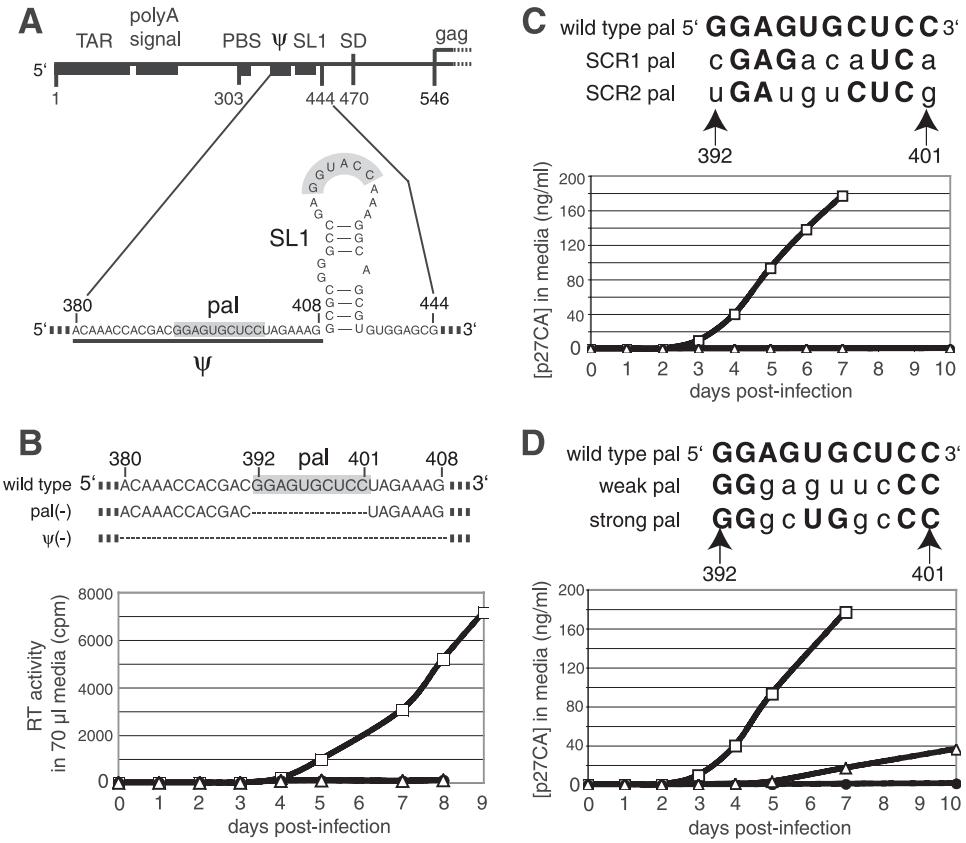

FIG. 1. 5′ leader region of HIV-2 ROD genomic RNA and mutations in the encapsidation domain. (A) The landmark sequences with known functions are indicated by boxes, with their names indicated above. TAR, polyA signal, PBS, ψ, SL1, SD, and *gag* represent the transactivation region, the poly(A) signal domain, the primer binding site, the encapsidation signal, stem-loop 1, the major splice donor site, and the 5′ end of the Gag protein coding region, respectively. The secondary structure of nucleotides 380 to 444 is represented, with gray boxes highlighting the 10-nt palindromic sequence pal and the 6-nt palindromic sequence in the loop of the SL1 element. The short thick line below nt 380 to 408 represents the encapsidation signal ψ characterized in cell culture (15). (B) Replication kinetics of wild-type (open squares), ψ-negative (open triangles), and pal-negative (closed circles) viruses in C8166 cells. DNA plasmids were transfected into COS-7 cells, and viruses were isolated from the supernatant. A standardized amount of viral particles (10 ng of p27 capsid, as determined by ELISA) was used to infect permissive C8166 cells. Aliquots of supernatants were then assayed for reverse transcriptase activity. (C) (Top) Sequences of the wild-type and scrambled pal 392-401 regions for the clones used in this experiment. SCR1 was designed to both destroy the palindrome and disrupt a proposed ψ-SL1 interaction (23, 24). SCR2 is the complementary sequence to SCR1. The nucleotides different from the wild-type sequence are represented with lowercase letters. (Bottom) Replication kinetics of wild-type (open squares), SCR1 (open triangles), and SCR2 (closed circles) pal viruses in C8166 cells. DNA plasmids were transfected into COS-7 cells, and viruses were isolated from the supernatant. A standardized amount of viral particles (10 ng of p27 capsid, as determined by ELISA) was used to infect permissive C8166 cells. Aliquots of supernatants were then assayed for p27 capsid by ELISA. (D) (Top) Sequences of the wild-type and mutated pal 392-401 regions for the clones used in this experiment. Weak and strong pal sequences were chosen from in vitro studies in which they were shown to form weaker and stronger RNA-RNA duplexes, respectively, than the wild-type sequence (36). (Bottom) Replication kinetics of wild-type (open squares), weak (open triangles), and strong (closed circles) pal viruses in C8166 cells. Viral replication was followed as described for panel C.

ment. Our results provide evidence for the existence of a structurally extended SL1 during HIV-2 replication, formed by the interaction of the 3′ end of the 10-nt pal element in ψ with a motif located downstream of SL1. Our observations also suggest that formation of the extended SL1 during viral replication positively affects HIV-2 genomic RNA encapsidation, although a palindromic sequence is not strictly required for viral viability.

MATERIALS AND METHODS

Plasmid construction. To engineer mutations in the 5′-untranslated region, we used a plasmid derived from a modified pROD10 plasmid containing full-length HIV-2 ROD (17, 42). The modified plasmid pROD10 was provided by the EU Programme EVA/MRC Centralised Facility for AIDS Reagents, NIBSC, United Kingdom. The AatII-XhoI fragment from modified pROD10 digestion was subcloned into pGEM7-Zf+ (Promega). This plasmid contains the 5′ long terminal repeat and most of the *gag* coding region (Fig. 1) (22). The numbering is based on the genomic RNA sequence of an HIV-2 ROD isolate (GenBank accession no. M15390). Most mutations were introduced using a QuikChange II XL site-directed mutagenesis kit (Stratagene) and the appropriate primers. The reversion-associated mutations in the ψ-SL1 region were introduced using a QuikChange II XL kit with plasmids bearing the original mutations. The AatII-XhoI fragments of plasmids bearing the mutations were then reinserted in the modified pROD10 backbone. All constructs were checked by DNA sequencing.

Cell culture and transfection. COS-7 cells were maintained in Dulbecco's modified Eagle's medium supplemented with 10% fetal calf serum, penicillin, and streptomycin (Invitrogen). Transient transfection of COS-7 cells was performed using a Trans-IT-COS transfection kit (Mirus). Cells and medium were harvested at 2 days posttransfection. HIV-2 capsid protein levels in the medium

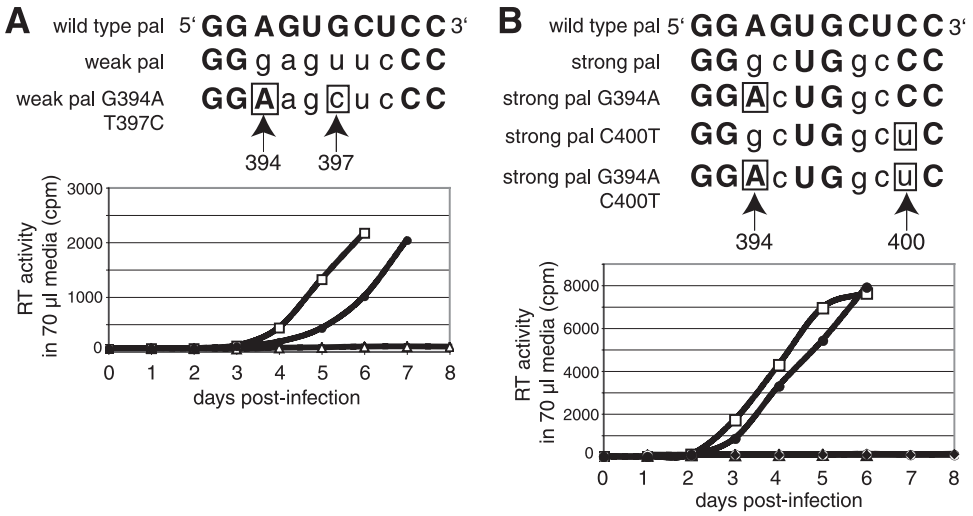

FIG. 2. Two nucleotide changes that appeared during long-term culture are solely able to restore viral replication in alternative ψ(pal) viruses. (A) (Top) Sequences of the wild-type, weak, and weak G394A/T397C mutant pal 392-401 regions for the clones used in this experiment. The reversion-associated mutations are boxed, and nucleotides different from the wild-type sequence are shown with lowercase letters. (Bottom) Replication kinetics of wild-type (open squares), weak (open triangles), and weak G394A/T397C mutant (closed circles) pal viruses in C8166 cells. Viral replication was followed as described in the legend to Fig. 1B. (B) (Top) Sequences of the wild-type and mutated pal 392-401 regions for the clones used in this experiment. (Bottom) Replication kinetics of wild-type (open squares), strong (closed diamonds), strong G394A mutant (closed triangles), strong C400T mutant (open circles), and strong G394A/C400T mutant (closed circles) pal viruses in C8166 cells. Viral replication was followed as described in the legend to Fig. 1B.

were quantified by a p27-specific enzyme-linked immunosorbent assay (SIV p27 ELISA; Zeptometrix). The infectivity of viruses in the medium was quantified using P4-CCR5 indicator cells. This cell line expresses the CD4 and CCR5 receptors and contains a beta-galactosidase gene under the control of the HIV long terminal repeat, thus detecting synthesis of the transactivating Tat protein after productive infection of the cells by the input viruses (5). After 2 days of culture postinfection, the cells were stained for beta-galactosidase activity, and the blue infected cells were counted. The numbers were then normalized first to the amounts of input viruses, as determined by reverse transcriptase activities, and second to the level of infection by wild-type (wt) virus to give the infectivities of viruses relative to the wild type.

Cell culture and infection. C8166 cells (NIH AIDS reagent 404) were maintained in Roswell Park Memorial Institute (RPMI) 1640 medium supplemented with 10% fetal calf serum, penicillin, streptomycin, and glutamine (Invitrogen). Medium from transfected COS-7 cells containing 10 ng of HIV-2 p27 capsid protein, as determined by ELISA, was used to infect 2×10^4 C8166 cells. This corresponds to a multiplicity of infection of 0.01 for the wild-type virus, as determined with P4-CCR5 indicator cells (data not shown). After 12 h, cells were washed twice and resuspended in RPMI medium-fetal calf serum. An aliquot of medium was then taken and served as a reference (p27 ELISA). Aliquots of medium were taken daily and spun to remove cells, and the supernatants were frozen at −80°C. Viral replication was followed for 1 or 2 weeks by quantifying the level of either CAp27 protein or reverse transcriptase activity in the supernatant. The CAp27 protein concentration was determined by enzyme-linked immunosorbent assay (Zeptometrix). The level of reverse transcriptase activity was quantified using the Amersham Biosciences Quan-T-RT assay system.

RNA isolation and analysis. The total cellular RNA and the extracellular viral RNA fractions were purified using a Stratagene Absolutely RNA RT-PCR miniprep kit. To pellet the viral particles, a fraction of the medium was centrifuged for 2 hours at 4°C and 12,000 rpm. Purified RNAs were used for reverse transcription-PCR (AccuScript high-fidelity RT-PCR system; Stratagene) or an RNase protection assay (RPA III; Ambion), as described by the manufacturer. Briefly, the RNase protection assay was done using an antisense RNA probe complementary to the region of positions 401 to 562 of the HIV-2 ROD isolate. The antisense region was cloned into the pGEM7Zf(+) vector (Novagen) so that the T7 transcript had around 45 nucleotides of vector at its 5′ end. The non-HIV-2 tail of the probe was used as a marker of the RNase's digestion efficiency during the RNase protection experiment. Up to two protected bands were expected, with a 162-nt band corresponding to the 5′ end of the unspliced genomic RNA and a 70-nt band corresponding to any spliced HIV-2 RNAs (see Fig. 3B). Furthermore, targeting of the region of positions 401 to 562 gives the same profile with wild-type or pal-mutated viral RNAs.

RESULTS

Identification of a conserved 10-nucleotide palindromic sequence in the core ψ region of HIV-2 leader RNA. The region located upstream of the HIV-2 SL1 element is able to influence the SL1-mediated dimerization of leader RNA fragments in vitro (23). We therefore wanted to assess its functional importance in HIV-2 replication in cell culture. We deleted the 10-nt palindromic sequence (pal) located upstream of SL1 and in the downstream part of the encapsidation signal ψ characterized by Lever and colleagues (Fig. 1A) (15). Infection of permissive C8166 cells by both ψ-negative and pal-negative mutants did not lead to productive infection, suggesting that an important functional element overlaps with the 10-nt palindromic sequence (Fig. 1B).

Since deletion of the 10-nt pal greatly affected viral replication, we then analyzed the effects of substitutions that destroy the palindromic nature of the pal element on viral replication (Fig. 1C). Despite robust virus production after transfection in COS-7 cells (data not shown), SCR1 and SCR2 mutants were defective for replication in permissive C8166 cells (Fig. 1C).

We chose to further test whether the palindromic nature of pal may play a role in virus replication in cell culture. We constructed two substitution mutants (Fig. 1D) that we call strong pal (5′-GGGCUGGCCC-3′) and weak pal (5′-GGGA GUUCCC-3′). These sequences have been shown to form stronger or weaker RNA-RNA duplexes (compared to the wt sequence) in vitro (36). Infection of permissive C8166 cells by strong and weak pal mutant viruses did not lead to productive

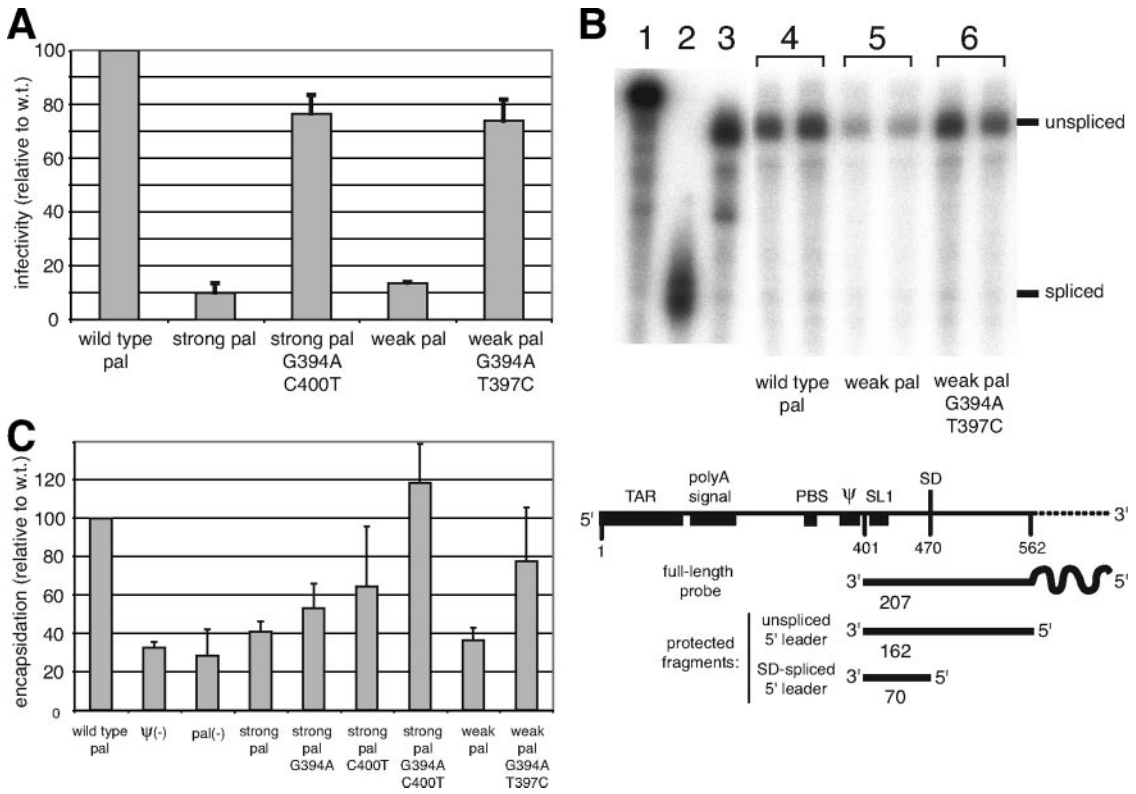

FIG. 3. Infectivity and genomic RNA encapsidation are affected by alternative ψ(pal) mutations and restored through reversion-associated mutations. (A) Single-round infectivity assay with P4-CCR5 reporter cells of viruses produced by transfected COS-7 cells. The mutated viruses used in this experiment are shown in Fig. 2. The infectivity assay is described in Materials and Methods. The error bars represent the standard deviations for duplicate experiments. (B) (Top) RNase protection assay of wild-type (lanes 4), weak (lanes 5), and weak G394A/T397C mutant (lanes 6) pal viruses. The controls were the undigested probe (lane 1) and the digested probe used with in vitro RNA transcript 1-470 (lane 2) or 1-561 (lane 3). (Bottom) Diagram of the radioactive antisense probe used in this experiment and the expected protected fragments. (C) Encapsidation yields of different pal-mutated viruses. The amounts of unspliced genomic RNA in viruses isolated from the medium of transfected COS-7 cells were quantified using an RNase protection assay. The numbers were then normalized first to the amount of viruses in the medium, as determined by p27 capsid ELISA, and second to the level of encapsidation by wild-type viruses, set at 100%, to give the encapsidation relative to that of the wild type. The error bars represent the standard deviations for two or three experiments.

infections relative to wild-type infections, with weak pal and strong pal viruses showing low or no virus production (Fig. 1D). These results indicate that the palindromic nature of pal is perhaps less important than its primary sequence for HIV-2 replication in cell culture.

Phenotypic reversion of alternative pal mutants in long-term culture. In order to see if the replication of the defective viruses could be enhanced by virus-induced mutations, duplicates of the SCR2, strong, and weak pal virus cultures shown in Fig. 1C and 1D were passaged for several months. During the first several weeks of culture, no cytopathic effects were observed for any of the viruses. However, cell death and syncytia were observed at around 8 weeks postinfection for the weak pal cultures and at week 14 for one of the strong pal cultures. The supernatants of these three cultures tested positive for both reverse transcriptase activity and the presence of the p27 capsid antigen. However, the SCR2 pal cultures never reverted, and neither viral proteins nor viral RNA or DNA could be detected outside or inside the cells after 8 months of culture (data not shown).

Aliquots of infected cells were harvested at week 15 postinfection, and the region corresponding to the leader of the genomic RNA was sequenced after RT-PCR to check the sequence variability in the pool of infected cells for each culture (Table 1). Aliquots of supernatants were also harvested at week 26 and processed similarly. Despite the presence of T310 in all of the original plasmid DNAs, all sequences showed a majority of T310C nucleotide changes in the primer-binding site after extended culture (data not shown), which indicates that a $tRNA_3^{Lys}$ molecule was used as the primer for reverse transcription, rather than $tRNA_5^{Lys}$ (8).

Interestingly, the other nucleotide changes in the 5′-untranslated region were located in or close to the mutated pal region. One reversion to a wild-type nucleotide was seen in all clones: the mutation A394G in the pal domain reverted back to A394 (Table 1). Two other nucleotide changes were seen in or downstream of the mutated pal region: C400 changed to T400 for the strong pal culture by week 15, and a partial or total change of G442 to A442 occurred in the weak pal cultures between weeks 15 and 26 (Table 1).

Effects of reversion-associated mutations in the weak and strong pal regions on viral replication. To test if the mutations we observed in the mutated pal regions of the phenotypically reverted clones were solely responsible for the re-

TABLE 1. Changes in the ψ-SL1 region occurring during long-term culture of strong and weak pal-defective viruses

Virus	Time of culture (wk)	Nucleotide at indicated position			
		394	397	400	442
Wild type		A	G	C	G
Strong pal 1[a]	0	G	G	C	G
	15	G > A[b]	G	T	G
	26	A	G	T	G
Weak pal 1	0	G	T	C	G
	15	A	T	C	G
	26	A	T > C[b,c]	C	G > A[b,c]
Weak pal 2	0	G	T	C	G
	15	A	T	C	A > G[b]
	26	A	T	C	A ≫ G[b]

[a] The strong pal 2 culture never reverted.
[b] The proportion of each nucleotide was estimated according to the areas of the peaks of corresponding nucleotides on the sequencing electropherogram.
[c] Twenty-two individual clones were sequenced. Among these 22 clones, the distribution of pairs at positions 397 and 442 was as follows: TG = 2, TA = 16, CG = 4, and CA = 0.

versions, we cloned these changes into the original weak or strong pal HIV-2 DNA backbone. We tested one of the three different reversion-associated mutation sets identified by the sequencing of individual clones, namely, two nucleotide changes in the weak pal region (G394A and T397C) (Table 1 and Fig. 2A). The medium from the resulting COS-7 transfection was used to infect C8166 cells, using a constant amount of p27 capsid, as measured by ELISA. The two nucleotide changes in the weak pal domain (G394A and T397C) increased the levels of viral replication of the mutated weak pal viruses to close to the wild-type level (Fig. 2A). This conclusion held true for the two nucleotide changes in the strong pal domain, i.e., G394A and C400T (Table 1 and Fig. 2B). The changes increased the level of viral replication of the strong pal G394A/C400T virus to close to the wild-type level (Fig. 2B). Interestingly, none of the single changes was able to compensate for the defective replication of strong pal viruses (Fig. 2B). Only when the G394A and C400T nucleotide changes were present in the same genomic RNA were the mutated viruses able to replicate at or close to the wild-type level (Fig. 2B). Thus, two nucleotide changes in the weak and strong pal domains were able to restore viral replication efficiency.

Effects of reversion-associated mutations in the weak and strong pal regions on genomic RNA encapsidation. We then sought to identify the stage(s) of HIV-2 replication in C8166 cells responsible for the low replication levels of the weak and strong pal viruses and for the wt level of the weak and strong pal viruses containing the two reversion-associated nucleotide changes, i.e., G394A/T397C and G394A/C400T, respectively (Fig. 2). First, the phenotypes observed in C8166 cell cultures were also observed when the viruses were tested on P4-CCR5 reporter cells (Fig. 3A), underscoring the gravity of the defect(s). Second, we used an RNase protection assay to detect the level of genomic RNA encapsidation, since the pal element is located in a sequence, ψ, that has been shown to play an important role in encapsidation (15). The encapsidation of ψ-negative and pal-negative genomic RNAs was similarly decreased threefold relative to the wt level (Fig. 3C). Indeed, the encapsidation level of weak pal genomic RNA in COS-7-produced virions was also decreased two- to threefold (Fig. 3B and C). Importantly, the genomic RNA encapsidation level for the weak pal G394A/T397C virus was at or close to the wild-type level (Fig. 3B and C). Similar results were found for the strong pal and strong pal G394A/C400T viruses (Fig. 3C). The single changes (G394A or C400T) partially increased the encapsidation levels of the corresponding genomic RNA molecules, suggesting a cumulative effect of both nucleotide changes when present in the same genomic RNA (Fig. 3C). Thus, two nucleotide changes in the weak and strong pal domains were able to compensate for the drop in genomic RNA encapsidation.

DISCUSSION

An impetus for this study was derived from prior in vitro studies of functional interactions in the HIV-2 leader RNA. We and others showed evidence that several short- and long-distance interactions in the HIV-2 leader RNA influence the presentation of the SL1 dimerization element in vitro (10, 24). Secondary structure prediction suggested a base-pairing interaction between the 5′ end of SL1 and a sequence immediately upstream, which could be responsible for the functional silencing of SL1-mediated leader RNA dimerization (24). The nature of this silencer sequence was interesting for two reasons. First, it is located in the downstream part of the encapsidation signal ψ characterized by Lever and colleagues (15). Second, it is a 10-nt palindromic (or autocomplementary) sequence which is phylogenetically conserved in HIV-2 and macaque and sooty mangabey SIVs (27).

In this work, we used long-term culture of defective viruses and their phenotypic reversion to study the functional importance of the 10-nt ψ pal in HIV-2 replication. In particular, we showed that the defects in viral replication for some pal-mutated viruses could be compensated for by two nucleotide changes in or close to the mutated pal element. The simplest way to explain the reversion results is to suppose that the 3′ end of the pal element is involved in an extended stem-loop 1 structure. Furthermore, characterization of the mutant viruses suggests that the formation of this extended structure is necessary for HIV-2 replication and affects genomic RNA encapsidation. The results also suggest that the 5′ end of the pal element plays a related but independent function to that of the 3′ end in viral replication and encapsidation. Furthermore, the fact that pal-mutated viruses lacking a functional palindromic sequence can replicate as well as wild-type pal viruses in C8166 cells suggests that the conservation of the pal element may be due more to its role in the formation of an extended stem-loop 1 structure than to a strict requirement for a palindrome.

The experiments presented here suggest a model for an essential function of the 3′ end of the pal element (GCUCC-3′) in the formation of a stem with a 5′-GGAGC element located downstream of SL1. We call the new stem extending the SL1 structure "stem B" because of its homology to that described for HIV-1 isolates (Fig. 4) (26, 43, 44). Indeed, the extended SL1 structure in HIV-2 was first proposed based on observed encapsidation and viral replication defects when larger deletions were made in the ψ-SL1 region (32). Recent computa-

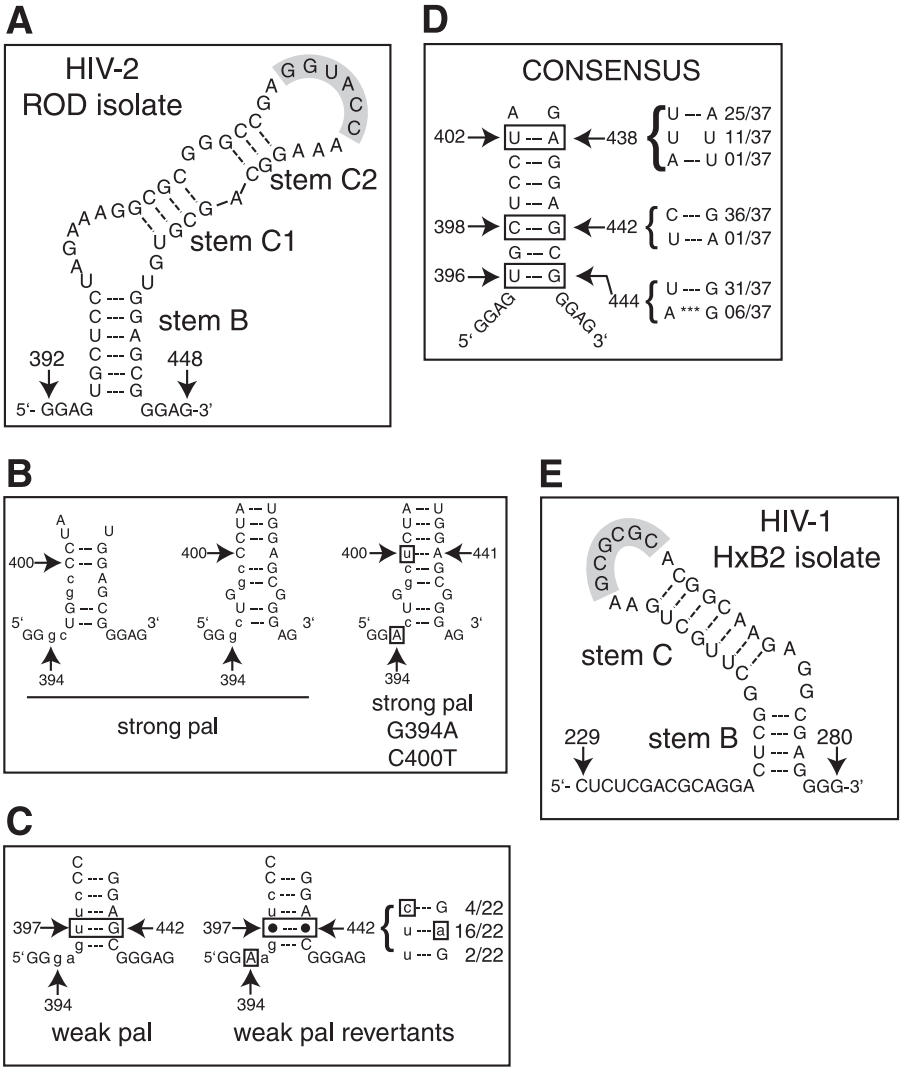

FIG. 4. Secondary structure models of extended SL1 and stem B structures described in this work. (A) The HIV-2 ROD isolate (GenBank accession no. M15390) SL1 structure is represented with another stem structure that base pairs with the 3′ end of the pal element with a 5′-GGAG-containing motif located immediately downstream of the short SL1 structure. We chose the names stem B and stems C1 and C2 to describe the extended HIV-2 SL1 in comparison with the structure of the HIV-1 SL1 element, as described by Laughrea and colleagues (26). (B) Mutations in the pal elements of strong pal viruses disrupt stem B (left structure). An alternative, more stable base pairing is possible by a one-nucleotide shift with a single mismatch in the middle (middle structure). The reversion-associated mutation C400T stabilizes the alternative stem B, and the G394A mutation restores a partial GGA motif (right structure). (C) Mutations in the pal elements of weak pal viruses decrease the stability of stem B (left structure). The reversion-associated mutation T397C or G442A stabilizes the mutated stem B by restoring Watson-Crick base pairing, while G394A reversion restores a partial GGA motif (right structure). The reversion-associated mutations are boxed, and nucleotides different from the wild-type sequence are shown with lowercase letters. (D) The consensus stem B structure from the analysis of 37 HIV-2 and SIV sequences from the *HIV Sequence Compendium 2005* is indicated, with the proportions of alternative base pairs shown to the right (27). (E) Secondary structure model of HIV-1 SL1 from the HxB2 isolate (GenBank accession no. K03455). The stems are named according to reference 26.

tional (21) and biochemical (7) analyses of the structure of the HIV-1 leader region further supported the existence of the stem B structure in SL1. Phylogenetic data provide evidence for the existence and conservation of stem B in HIV-1 (7, 21) and HIV-2 (Fig. 4D) (27).

The formation of stem B is an important step in HIV-2 replication. A less stable or nonexistent stem leads to a very low level of replication (Table 2) (ΔG values for wild-type, weak, and strong pal stems were −7.9, −3.7, and −4.1 kcal/mol, respectively), and genomic RNA encapsidation appears to be one of the stages affected by mutations in this region (Fig. 3C). The stem B-stabilizing reversion-associated mutations occurred at both wild-type nucleotides (Table 1) (strong pal C400T and weak pal G442A mutants) and at one originally mutated nucleotide (Table 1) (weak pal T397C mutant). The strong pal C400T reversion exchanged a CA for a UA base pair, increasing the stem stability from −4.1 to −8.3 (Fig. 4B and Table 2), while the weak pal T397C reversion replaced a wobble UG with a CG base pair, increasing the stem B stability from −3.7 to −6.2 (Fig. 4C and Table 2).

TABLE 2. Calculated ΔG values (kcal/mol) for putative pal-pal and stem B structures for the different sequences described in this work[a]

Virus	ΔG (kcal/mol)	
	pal-pal	Stem B
Wild type	−13.7	−7.9
Mutants		
ψ-negative mutant	NA	None
pal-negative mutant	NA	−2.7[b]
SCR1	−2.5	−3.3
SCR2	−4.7	None
Strong pal	−17.9	−4.1
Strong pal G394A	−6.3	−4.1
Strong pal C400T	−12.9	−8.3
Strong pal G394A/C400T	−4.1	−8.3
Weak pal	−11.2	−3.7
Weak pal G394A	−8.5	−3.7
Weak pal G442A	−11.2	−4.1
Weak pal T397C	−18.5	−6.2
Weak pal G394A/T397C	−6.5	−6.2
Weak pal G394A/G442A	−8.5	−4.1
HIV-1 HxB2		−1.9

[a] The calculations were done using the two-state hybridization model in the DINAmelt server (http://www.bioinfo.rpi.edu/applications/hybrid/twostate.php), using standard parameters (RNA at 37°C, $[Na^+] = 1$ M, $[Mg^{2+}] = 0$ M, and [strand] = 0.00001 M) (29). NA, not applicable.

[b] Alternative base pairing.

The importance of the 5′ end of the pal element is underscored by several points. First, most, but not all, pal-mutated viruses with wt stability for stem B replicated at wt levels (compare Fig. 1 and 2 to Table 2). Second, strong pal viruses bearing the single C400T change have a stem B stability similar to that of the wt, but they did not replicate in C8166 cells. They showed an increased encapsidation level relative to the strong pal parent, but it was lower than the wt level (compare Fig. 2B and 3C and Table 2). Lastly, all of the phenotypically reverted viruses showed reversion of the G394 nucleotide back to the wild-type A394 nucleotide (Table 1). We hypothesize that the 5′ end of pal (5′-GGAG motif) is a purine-rich Gag polyprotein recognition element, which could be functionally related to the 5′-GGAG in HIV-1 SL3 (9). Indeed, purine-rich elements have a long history in retroviral RNA encapsidation and dimerization research (for example, see references 30 and 47), although their exact mode of action is not completely understood. In HIV-1, the purine-rich motifs in or downstream of SL3 play an important role in dimerization and encapsidation of the genomic RNA (40).

Remarkably, the phenotypic reversions we observed in our long-term culture experiments show that mutant viruses are viable without a palindromic sequence (compare Fig. 2 and Table 2), but it is not known if the mutated viruses would be viable in animal infections in vivo. The palindromic nature of pal is conserved in HIV-2 and SIV: 31 of 37 sequences examined show a T396-containing pal, whereas 6 sequences show an A396-containing pal (Fig. 4D) (27). The A396-containing pal isolates belong to HIV-2 type AB or B or SIV_{SMM} (27). The presence of A396, while setting up an AG base pair, is not at odds with the stem B model, as AG base pairs are frequently found at the ends of helices, where they form "conformationally unique helix extensions" (12). Indeed, it is possible that an A396-containing stem B could be slightly more stable than a U396-containing stem B, since the UG base pair in stem B is identified as a class B, "unstacked" pair which may not even base pair and, if it does, is probably not in a wobble conformation (13).

Although we cannot rule out that a pal-pal interaction between two HIV-2 RNA molecules exists transiently during viral replication, we now view the palindromic nature of pal as a fortuitous event in relation to the functions it fulfills: its 5′-GGAG(U) motif is likely to be a Gag polyprotein binding motif, while its GCUCC-3′ motif base pairs with another 5′-GGAG(C) motif downstream of SL1 to form stem B (Fig. 4A). The stem B of HIV-1 SL1 is also formed by a similar interaction between CUCG-3′ and 5′-CGAG motifs (compare stems B in Fig. 4A and E).

Finally, the finding of stem B extending the SL1 structure in HIV-2 genomic RNA brings both answers and exciting questions. The next endeavor will be to test if HIV-2 stem B is also involved in genomic RNA dimerization and reverse transcription, two functions that are naturally linked to this region (44). It will be equally intriguing to ascertain whether the formation of the extended SL1 during HIV-2 replication affects (or is affected by) the translation of the *gag* gene, since the absence or presence of the long-distance interaction involving the *gag* initiation codon seems to influence the presentation of the pal-SL1 domain in vitro (10, 24).

ACKNOWLEDGMENTS

This work was funded by National Institutes of Health grant AI45388 to J.S.L.

Anti-HIV-2 serum and C8166 cells were obtained through the AIDS Research and Reference Reagent Program, Division of AIDS, National Institutes of Health (no. 1030 and 404, respectively). The plasmid pROD10 was provided by the EU Programme EVA/MRC Centralised Facility for AIDS Reagents, NIBSC, United Kingdom (grant numbers QLK2-CT-1999-00609 and GP828102). We thank Kathryn Follis and Jack Nunberg from the University of Montana for assistance with the virological experiments. We also thank Tayyba Baig for critically reading the manuscript.

REFERENCES

1. **Arya, S. K., M. Zamani, and P. Kundra.** 1998. Human immunodeficiency virus type 2 lentivirus vectors for gene transfer: expression and potential for helper virus-free packaging. Hum. Gene Ther. **9:**1371–1380.
2. **Bender, W., and N. Davidson.** 1976. Mapping of poly(A) sequences in the electron microscope reveals unusual structure of type C oncornavirus RNA molecules. Cell **7:**595–607.
3. **Berkhout, B.** 1996. Structure and function of the human immunodeficiency virus leader RNA. Prog. Nucleic Acid Res. Mol. Biol. **54:**1–34.
4. **Berkowitz, R. D., M. L. Hammarskjold, C. Helga-Maria, D. Rekosh, and S. P. Goff.** 1995. 5′ regions of HIV-1 RNAs are not sufficient for encapsidation: implications for the HIV-1 packaging signal. Virology **212:**718–723.
5. **Charneau, P., M. Alizon, and F. Clavel.** 1992. A second origin of DNA plus-strand synthesis is required for optimal human immunodeficiency virus replication. J. Virol. **66:**2814–2820.
6. **Clever, J. L., D. Mirandar, Jr., and T. G. Parslow.** 2002. RNA structure and packaging signals in the 5′ leader region of the human immunodeficiency virus type 1 genome. J. Virol. **76:**12381–12387.
7. **Damgaard, C. K., E. S. Andersen, B. Knudsen, J. Gorodkin, and J. Kjems.** 2004. RNA interactions in the 5′ region of the HIV-1 genome. J. Mol. Biol. **336:**369–379.
8. **Das, A. T., M. Vink, and B. Berkhout.** 2005. Alternative tRNA priming of human immunodeficiency virus type 1 reverse transcription explains sequence variation in the primer-binding site that has been attributed to APOBEC3G activity. J. Virol. **79:**3179–3181.
9. **De Guzman, R. N., Z. R. Wu, C. C. Stalling, L. Pappalardo, P. N. Borer, and M. F. Summers.** 1998. Structure of the HIV-1 nucleocapsid protein bound to the SL3 psi-RNA recognition element. Science **279:**384–388.
10. **Dirac, A. M., H. Huthoff, J. Kjems, and B. Berkhout.** 2002. Regulated HIV-2 RNA dimerization by means of alternative RNA conformations. Nucleic Acids Res. **30:**2647–2655.

11. **D'Souza, V., and M. F. Summers.** 2005. How retroviruses select their genomes. Nat. Rev. Microbiol. **3:**643–655.
12. **Elgavish, T., J. J. Cannone, J. C. Lee, S. C. Harvey, and R. R. Gutell.** 2001. AA.AG@helix.ends: A:A and A:G base-pairs at the ends of 16 S and 23 S rRNA helices. J. Mol. Biol. **310:**735–753.
13. **Gautheret, D., D. Konings, and R. R. Gutell.** 1995. G.U base pairing motifs in ribosomal RNA. RNA **1:**807–814.
14. **Greatorex, J., and A. Lever.** 1998. Retroviral RNA dimer linkage. J. Gen. Virol. **79:**2877–2882.
15. **Griffin, S. D., J. F. Allen, and A. M. Lever.** 2001. The major human immunodeficiency virus type 2 (HIV-2) packaging signal is present on all HIV-2 RNA species: cotranslational RNA encapsidation and limitation of Gag protein confer specificity. J. Virol. **75:**12058–12069.
16. **Guan, Y., J. B. Whitney, K. Diallo, and M. A. Wainberg.** 2000. Leader sequences downstream of the primer binding site are important for efficient replication of simian immunodeficiency virus. J. Virol. **74:**8854–8860.
17. **Guyader, M., M. Emerman, P. Sonigo, F. Clavel, L. Montagnier, and M. Alizon.** 1987. Genome organization and transactivation of the human immunodeficiency virus type 2. Nature **326:**662–669.
18. **Haddrick, M., A. L. Lear, A. J. Cann, and S. Heaphy.** 1996. Evidence that a kissing loop structure facilitates genomic RNA dimerisation in HIV-1. J. Mol. Biol. **259:**58–68.
19. **Hoglund, S., A. Ohagen, J. Goncalves, A. T. Panganiban, and D. Gabuzda.** 1997. Ultrastructure of HIV-1 genomic RNA. Virology **233:**271–279.
20. **Jewell, N. A., and L. M. Mansky.** 2000. In the beginning: genome recognition, RNA encapsidation and the initiation of complex retrovirus assembly. J. Gen. Virol. **81:**1889–1899.
21. **Kasprzak, W., E. Bindewald, and B. A. Shapiro.** 2005. Structural polymorphism of the HIV-1 leader region explored by computational methods. Nucleic Acids Res. **33:**7151–7163.
22. **Kaye, J. F., and A. M. Lever.** 1998. Nonreciprocal packaging of human immunodeficiency virus type 1 and type 2 RNA: a possible role for the p2 domain of Gag in RNA encapsidation. J. Virol. **72:**5877–5885.
23. **Lanchy, J. M., J. D. Ivanovitch, and J. S. Lodmell.** 2003. A structural linkage between the dimerization and encapsidation signals in HIV-2 leader RNA. RNA **9:**1007–1018.
24. **Lanchy, J. M., C. A. Rentz, J. D. Ivanovitch, and J. S. Lodmell.** 2003. Elements located upstream and downstream of the major splice donor site influence the ability of HIV-2 leader RNA to dimerize in vitro. Biochemistry **42:**2634–2642.
25. **Laughrea, M., and L. Jette.** 1996. Kissing-loop model of HIV-1 genome dimerization: HIV-1 RNAs can assume alternative dimeric forms, and all sequences upstream or downstream of hairpin 248-271 are dispensable for dimer formation. Biochemistry **35:**1589–1598.
26. **Laughrea, M., N. Shen, L. Jette, and M. A. Wainberg.** 1999. Variant effects of non-native kissing-loop hairpin palindromes on HIV replication and HIV RNA dimerization: role of stem-loop B in HIV replication and HIV RNA dimerization. Biochemistry **38:**226–234.
27. **Leitner, T., B. Foley, B. Hahn, P. Marx, F. McCutchan, J. Mellors, S. Wolinsky, and B. Korber.** 2005. HIV sequence compendium 2005. Theoretical Biology and Biophysics Group, Los Alamos National Laboratory, Los Alamos, NM.
28. **Mangel, W. F., H. Delius, and P. H. Duesberg.** 1974. Structure and molecular weight of the 60-70S RNA and the 30-40S RNA of the Rous sarcoma virus. Proc. Natl. Acad. Sci. USA **71:**4541–4545.
29. **Markham, N. R., and M. Zuker.** 2005. DINAMelt web server for nucleic acid melting prediction. Nucleic Acids Res. **33:**W577–W581.
30. **Marquet, R., J. C. Paillart, E. Skripkin, C. Ehresmann, and B. Ehresmann.** 1994. Dimerization of human immunodeficiency virus type 1 RNA involves sequences located upstream of the splice donor site. Nucleic Acids Res. **22:**145–151.
31. **McBride, M. S., and A. T. Panganiban.** 1996. The human immunodeficiency virus type 1 encapsidation site is a multipartite RNA element composed of functional hairpin structures. J. Virol. **70:**2963–2973.
32. **McCann, E. M., and A. M. Lever.** 1997. Location of *cis*-acting signals important for RNA encapsidation in the leader sequence of human immunodeficiency virus type 2. J. Virol. **71:**4133–4137.
33. **Muriaux, D., P. Fosse, and J. Paoletti.** 1996. A kissing complex together with a stable dimer is involved in the HIV-1 Lai RNA dimerization process in vitro. Biochemistry **35:**5075–5082.
34. **Paillart, J. C., M. Shehu-Xhilaga, R. Marquet, and J. Mak.** 2004. Dimerization of retroviral RNA genomes: an inseparable pair. Nat. Rev. Microbiol. **2:**461–472.
35. **Paillart, J. C., E. Skripkin, B. Ehresmann, C. Ehresmann, and R. Marquet.** 1996. A loop-loop "kissing" complex is the essential part of the dimer linkage of genomic HIV-1 RNA. Proc. Natl. Acad. Sci. USA **93:**5572–5577.
36. **Pan, Y., U. D. Priyakumar, and A. D. MacKerell, Jr.** 2005. Conformational determinants of tandem GU mismatches in RNA: insights from molecular dynamics simulations and quantum mechanical calculations. Biochemistry **44:**1433–1443.
37. **Patel, J., S. W. Wang, E. Izmailova, and A. Aldovini.** 2003. The simian immunodeficiency virus 5′ untranslated leader sequence plays a role in intracellular viral protein accumulation and in RNA packaging. J. Virol. **77:**6284–6292.
38. **Poeschla, E., J. Gilbert, X. Li, S. Huang, A. Ho, and F. Wong-Staal.** 1998. Identification of a human immunodeficiency virus type 2 (HIV-2) encapsidation determinant and transduction of nondividing human cells by HIV-2-based lentivirus vectors. J. Virol. **72:**6527–6536.
39. **Rizvi, T. A., and A. T. Panganiban.** 1993. Simian immunodeficiency virus RNA is efficiently encapsidated by human immunodeficiency virus type 1 particles. J. Virol. **67:**2681–2688.
40. **Russell, R. S., J. Hu, V. Beriault, A. J. Mouland, M. Laughrea, L. Kleiman, M. A. Wainberg, and C. Liang.** 2003. Sequences downstream of the 5′ splice donor site are required for both packaging and dimerization of human immunodeficiency virus type 1 RNA. J. Virol. **77:**84–96.
41. **Russell, R. S., C. Liang, and M. A. Wainberg.** 2004. Is HIV-1 RNA dimerization a prerequisite for packaging? Yes, no, probably? Retrovirology **1:**23.
42. **Ryan-Graham, M. A., and K. W. Peden.** 1995. Both virus and host components are important for the manifestation of a Nef− phenotype in HIV-1 and HIV-2. Virology **213:**158–168.
43. **Shen, N., L. Jette, C. Liang, M. A. Wainberg, and M. Laughrea.** 2000. Impact of human immunodeficiency virus type 1 RNA dimerization on viral infectivity and of stem-loop B on RNA dimerization and reverse transcription and dissociation of dimerization from packaging. J. Virol. **74:**5729–5735.
44. **Shen, N., L. Jette, M. A. Wainberg, and M. Laughrea.** 2001. Role of stem B, loop B, and nucleotides next to the primer binding site and the kissing-loop domain in human immunodeficiency virus type 1 replication and genomic-RNA dimerization. J. Virol. **75:**10543–10549.
45. **Skripkin, E., J. C. Paillart, R. Marquet, B. Ehresmann, and C. Ehresmann.** 1994. Identification of the primary site of the human immunodeficiency virus type 1 RNA dimerization in vitro. Proc. Natl. Acad. Sci. USA **91:**4945–4949.
46. **Strappe, P. M., J. Greatorex, J. Thomas, P. Biswas, E. McCann, and A. M. Lever.** 2003. The packaging signal of simian immunodeficiency virus is upstream of the major splice donor at a distance from the RNA cap site similar to that of human immunodeficiency virus types 1 and 2. J. Gen. Virol. **84:**2423–2430.
47. **Sundquist, W. I., and S. Heaphy.** 1993. Evidence for interstrand quadruplex formation in the dimerization of human immunodeficiency virus 1 genomic RNA. Proc. Natl. Acad. Sci. USA **90:**3393–3397.